Available online at www.sciencedirect.com
SCIENCE DIRECT®
Journal of Power Sources 124 (2003) 505–512
JOURNAL OF POWER SOURCES
www.elsevier.com/locate/jpowsour

Effect of particle morphology on lithium intercalation rates in natural graphite

K. Zaghib [a,*], X. Song [b], A. Guerfi [a], R. Kostecki [b], K. Kinoshita [b]

[a] *Institut de Recherche d'Hydro-Québec (IREQ), 1800 boul, Lionel-Boulet, Varennes, Qué., Canada J3X 1S1*
[b] *Environmental Energy Technologies Division, Lawrence Berkeley National Laboratory, Berkeley, CA 94720, USA*

Received 28 May 2003; received in revised form 20 June 2003; accepted 20 June 2003

Abstract

The intercalation rate of Li^+-ions in flake natural graphite (two-dimensional) with particle size from 2 to 40 μm and sphere-like graphite (three-dimensional), 12 to 40 μm in particle size, was investigated. The amount of Li^+ ions that intercalate at different rates was determined from measurement of the reversible capacity during de-intercalation in 1 M $LiClO_4$/1:1 (volume ratio) ethylene carbonate—dimethyl carbonate. The key issues in this study are the role of the particle size and fraction of edge sites on the rate of intercalation and de-intercalation of Li^+ ions. At low specific current (15.5 mA/g carbon), the composition of lithiated graphite approaches the theoretical value, $x = 1$ in Li_xC_6, except for the natural graphite with the largest particle size. However, x decreases with an increase in specific current for all particle sizes. This trend suggests that slow solid-state diffusion of Li^+ ions limits the intercalation capacity in graphite. The 3D natural graphite with a particle size of 12 μm may provide the optimum combination of reversible capacity and irreversible capacity loss in the electrolyte and discharge rates used in this study.

Keywords: Lithium intercalation; Natural graphite; Particle size

1. Introduction

Lithium-ion batteries are now widely used in consumer electronic devices such as cellular telephones, camcorders and portable computers. There is now a strong interest in utilizing Li-ion batteries for transportation applications. The United States Advanced Battery Consortium (USABC) was formed in the early 1990s to develop large-scale rechargeable lithium batteries for consumer electric vehicles. This effort was followed by the formation of the Partnership for the New Generation Vehicle (PNGV), which has a goal of developing a passenger automobile that can achieve the equivalent of 80 mpg. Both the USABC and PNGV Programs supported the development of Li-ion batteries. One requirement of these Li-ion batteries is the capability to sustain high charge–discharge rates [1]. This requirement is particularly critical in hybrid electric vehicles for the PNGV Program. Because carbon is the usual host for storing Li^+ ions in the negative electrodes of Li-ion batteries, its ability to rapidly transport Li^+ ions is crucial for high-rate charge–discharge of these electrodes. With this in mind, we are investigating the charge–discharge characteristics of a series of flake-like natural graphite of different particle sizes. An analysis of the irreversible capacity loss [2] and thermal oxidation properties [3] of these natural graphite samples was presented earlier.

Theoretical analyses of intercalation electrodes have been conducted by a number of researchers [4–9]. These studies show that the particle size, particle surface area, solid-state and liquid-phase diffusion rates of intercalant ions, electrode thickness and electrode porosity can have a significant influence on the charge–discharge rates and utilization of intercalation electrodes. For example, Verbrugge and Koch [4] analyzed the charge-transfer reaction and diffusion of intercalants in porous electrodes. Their results are useful for analyzing the charge–discharge behavior of graphite electrodes for Li-ion batteries. They defined a parameter ζ that is a reflection of the relative importance of solid-state transport resistance to that of the liquid phase:

$$\zeta = \left[\frac{D_{\text{salt}}}{D_{\text{I}}^{\text{o}}}\right]\left[\frac{r_{\text{s}}}{L}\right]^2 \quad (1)$$

where D_{salt} is the salt diffusion coefficient, D_{I}^{o} the intercalant diffusion coefficient at infinite dilution, r_{s} the characteristic dimension of the particle, and L the thickness of the porous

* Corresponding author. Tel.: +1-450-652-8019; fax: +1-450-652-8424.
E-mail address: karimz@ireq.ca (K. Zaghib).

0378-7753/$ – see front matter © 2003 Elsevier B.V. All rights reserved.
doi:10.1016/S0378-7753(03)00801-2

electrode. When ζ is large, solution-phase diffusion resistance does not need to be considered. With typical values quoted by Verbrugge and Koch ($D_{salt} = 5.5 \times 10^{-6}$ cm^2/s, $D_I^o = 1 \times 10^{-10}$ cm^2/s, $r_s = 0.3\,\mu$m, $L = 20\,\mu$m), $\zeta = 12.375$, which suggests that only solid-state diffusion should be considered. Fuller et al. [6] also analyzed transport in solution and intercalation electrodes and defined a dimensionless parameter S_s that is a ratio of the diffusion time in the electrode to the discharge time. They concluded that diffusion limitations may exist in carbon in their analysis.

Studies of the charge–discharge rate capabilities of carbon particles considered for Li-ion batteries were reported in several publications. Tran et al. [10] observed that the lithium intercalation process is inherently slower than the de-intercalation process. This characteristic property appears to affect the capacity of graphite electrodes at various charge–discharge rates, especially when the discharge rate is not sufficiently slow to ensure complete intercalation. Electrode capacities are independent of charge (de-intercalation) rate when the electrode is fully intercalated. Fujimoto et al. [11] investigated the rate capabilities of natural graphite in a variety of mixed cyclic carbonate electrolytes: ethylene carbonate (EC), propylene carbonate (PC), butylene carbonate (BC), vinylene carbonate (VC), diethylcarbonate (DEC) and chloroethylene carbonate (CEC). The high-rate capability of natural graphite in VC/DEC was superior to that in other electrolytes, which was attributed to the higher conductivity of VC/DEC. Ogumi and co-workers [12] investigated the intercalation of Li^+ ions in natural graphite of different particle sizes by electrochemical impedance spectroscopy. They concluded that the charge-transfer reaction takes place on the whole surface of the graphite particles, but Li^+ ions intercalated only from the edge plane. Zhang [13] developed an expression for the rate capability and reversible capacity of carbon from cyclic voltammetry measurements. According to Zhang, intercalation of Li^+ ions is more difficult than de-intercalation in carbon electrodes, in agreement with the observation by Tran et al. [10]. Furthermore, the rate of intercalation tended to be slower in more highly crystalline carbons (i.e. graphite < soft carbon < hard carbon). These studies [10–13] provide some insight into the role of particle size on the charge–discharge rate of Li^+ ions in carbon particles. Liu et al. [14] reported that the particle size and particle size distribution of graphites have a great influence on their electrochemical performance in 1 M $LiClO_4$/ethylene carbonate (EC)—dimethyl carbonate (DMC). The intent of the present paper is to extend these studies by providing a systematic analysis of a series of natural graphite flakes with different morphologies (i.e. three- and two-dimension particles) but different average particle size.

2. Experimental

Six samples of flake natural graphite (two-dimensional) powders with average basal plane dimension of 2, 7, 12, 20, 30 and 40 μm were obtained from 350 μm particles by jet milling. The edge thickness of these samples ranged from 0.21 to 2.85 μm, as determined from measurements using scanning electron microscopy. The d_{002} spacing, which was determined by X-ray diffraction analysis, is 3.36 Å and is essentially the same for all of the samples. The jet mill process increases (see Fig. 1) the amount of 3R (Rombohedral) phase. Graphite with >30% 3R phase does not exfoliate in PC (propylene carbonate) based electrolyte. The 2H and 3R phases are dependent on the particle size. The basal length of the particles is taken to be the same dimension as the average particle size. The physical properties of these samples were summarized elsewhere [2]. Four samples of sphere-like natural graphite powders (three-dimensional) with average particle size of 12, 20, 30 and 40 μm (SNG12-SNG40) were obtained by jet milling and a process developed by Hydro-Quebec (3D process), The 3D mechanical process increases (see Fig. 2) the amount of 3R (Rombohedral) phase, with the 2H and 3R phase independent of particle size. The maximum length of the particles is taken to be the same dimension as the average particle size.

The working electrode was fabricated from a mixture of natural graphite and poly(vinylidene fluoride) (PVDF) dissolved in 1-methyl-2-pyrrolidinone (NMP). The slurry was spread onto a copper grid (Exmet Corp., Naugatuck, CT) and dried under vacuum at 95 °C for 24 h. A typical electrode thickness is about 200 μm, and the electrode area is 12 cm^2 (6 cm^2 per side). The working electrodes were evaluated in a three-electrode cell that contained metallic Li as both the counter and reference electrodes. The cells were built in a glove box under an Ar atmosphere containing less than 5 ppm humidity. Electrochemical measurements of the charge–discharge of graphite were conducted in an electrolyte containing 1 M $LiClO_4$ in 1:1 (volume ratio) EC-DMC (Tomiyama Pure Chemical Industries Ltd.). The cells were cycled between 2.5 and 0 V versus Li/Li^+ with a MacPile II (Bio Logic, France).

The electrochemical experiments involved the following procedure. The electrode is discharged (Li^+-ion intercalation) at *C*/24 to form a stable solid electrolyte interface (SEI) layer. A constant current is applied until the electrode potential reaches 0 mV, then the electrode is charged (Li^+ de-intercalation) at the *C*/24 rate. Following the formation cycle, the electrode is cycled to higher discharge rates corresponding to *C*/8, *C*/6, *C*/4, *C*/2 and 2*C*. Between each of the intercalation steps, the electrode is de-intercalated at the *C*/12 rate to 2.5 V prior to discharging to determine the reversible capacity. In these experiments, the reversible capacity of the natural graphite is determined as a function of discharge rate and particle size.

3. Discussion of results

Data analysis. Eq. (1), which was reported by Verbrugge and Koch [4], was used to determine the relative importance

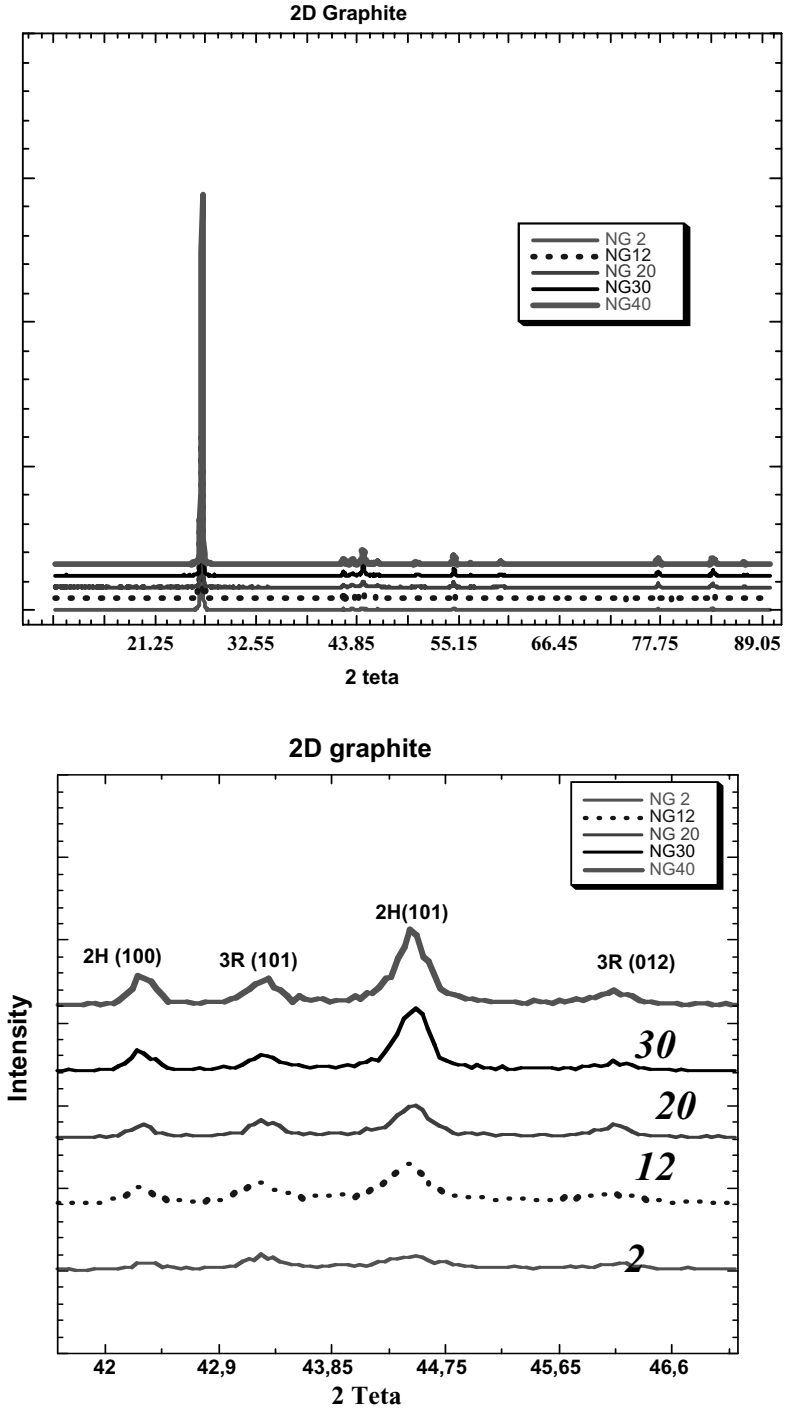

Fig. 1. X-ray diffraction patterns of 2D natural graphite NG2, NG12, NG20, NG30 and NG40.

of transport resistance in the solid state (graphite) to that of the liquid phase (electrolyte). Using the values quoted by Verbrugge and Koch ($D_{\text{salt}} = 5.5 \times 10^{-6}\,\text{cm}^2/\text{s}$, $D_{\text{l}}^{\text{o}} = 1 \times 10^{-10}\,\text{cm}^2/\text{s}$), we can determine ζ for the dimension of the natural graphite particles and electrode thickness used in our study. We take r_{s} to be in the range from 1 to 20 μm and L equal to 100 μm (1/2 of typical electrode thickness because both sides are accessible to the electrolyte), which yields ζ of 5.5 and 2200, respectively, for the two extreme values of r_{s}. Therefore, we concluded that solution-phase diffusion resistance is negligible, and the charge–discharge behavior is a function of solid-state transport of the intercalant, Li^+ ions. Verbrugge and Koch reached another conclusion regarding the ohmic resistance in the porous electrode. Their analysis showed that the ohmic resistance in the electrolyte and solid phases in the electrode were insignificant compared to the intercalant diffusion resistance in their study. A similar situation is expected in our experiments.

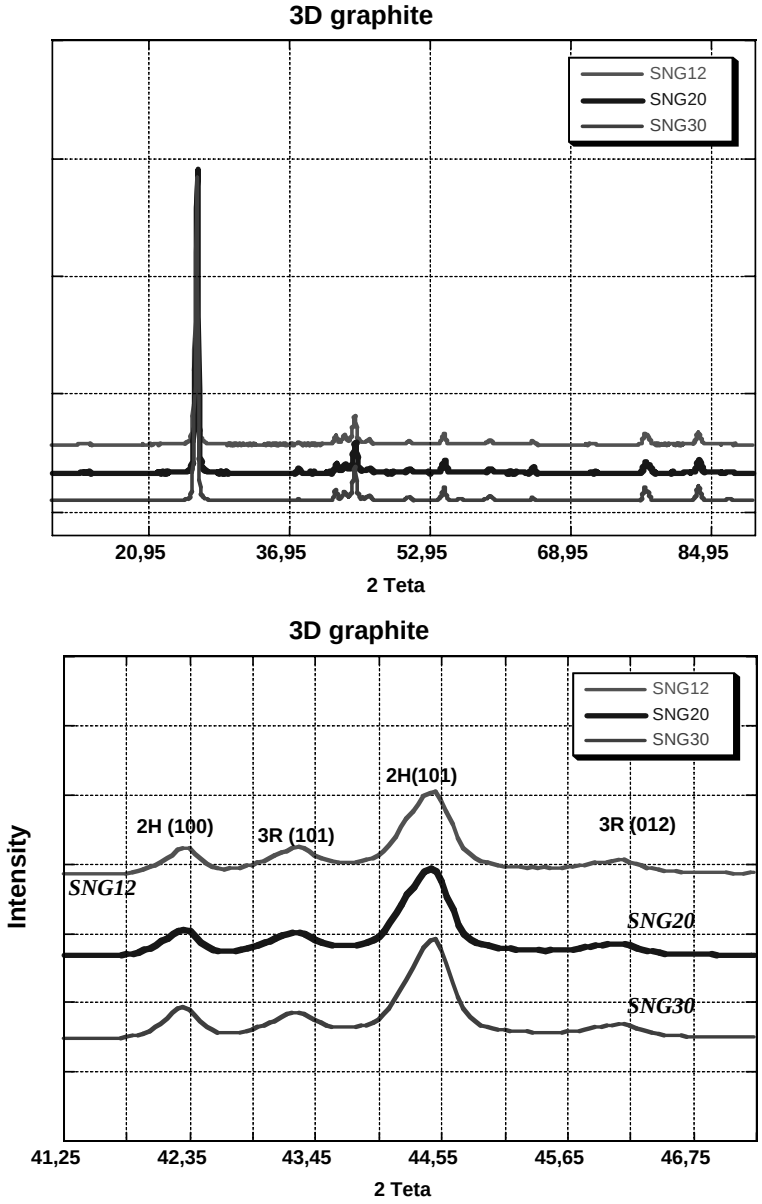

Fig. 2. X-ray diffraction patterns of 3D natural graphite SNG12, SNG20 to SNG30.

The key issues we considered in this study are the role of particle size and fraction of edge sites on the rate of intercalation and de-intercalation of Li^+ ions. The edge sites, and not the basal plane sites, are the graphite/electrolyte interfacial sites where insertion of Li^+ ions takes place to form the lithiated graphite. Lattice defects may be present on the basal plane that could also serve as insertion sites for Li^+ ions. The contribution of these sites for intercalation is considered to be negligible compared to that from the edge sites. The total area of edge sites (S_e) is a function of the surface area of graphite (S) and the fraction of edge sites (f_e):

$$S_e = f_e S \tag{2}$$

The surface area is measured experimentally, and f_e is computed from an equation derived by analysis of a model prismatic structure of graphite particle. Previously, a complex derivation of f_e was presented [4]. For the present discussion, a simplified approach is taken in which the edge surface area is estimated from the geometry of the particle morphology. The flux of intercalant ions occurs normal to the surface of the edge planes, thus it is assumed that the edge surface area can be estimated from the thickness and width of the edge planes. The flake graphite is assumed to have a prismatic shape (i.e. length(B) × width(B)) with thickness of the edge planes T, and basal plane dimension or particle size B. For this geometry, the edge area (EA) is given by

$$\mathrm{EA} = 4BT \tag{3}$$

and the basal plane area (BA) is

$$\mathrm{BA} = 2B^2 \tag{4}$$

Table 1
Analysis of fraction of edge sites on prismatic structure

Graphite sample	Particle size (B) (μm)	Edge thickness (T) (μm)	BET surface area (m^2/g)	Fraction of edge sites	Edge surface area (m^2/g)
NG2	2	0.21	12.0	0.17	2.1
NG7	7	0.59	5.1	0.14	0.7
NG12	12	0.49	4.3	0.08	0.3
NG20	20	1.54	3.2	0.13	0.4
NG30	30	2.03	2.6	0.12	0.3
NG40	40	2.85	2.3	0.12	0.3

The fraction of edge sites is obtained from Eqs. (3) and (4)

$$f_e = \frac{EA}{EA + BA} \quad (5)$$

The results of this analysis using Eq. (5) are summarized in Table 1. The fraction of edge sites varies from 0.17 for the smallest particles to 0.12 for the largest particles. The calculation for NG12 yields $f_e = 0.08$, which is considerable lower than the other values. This discrepancy arises from the low value of T.

The reversible capacity of graphite is equal to 372 mAh/g (equivalent to the composition LiC_6),

$$I_t t_t = 372 \quad (6)$$

where I_t is the specific current (mA/g carbon) and t_t the time for charge–discharge (i.e. equivalent to the C-rate). Atlung et al. [8] proposed a constant Q that is a measure of how fast solid-state transport is compared to the discharge rate of an intercalation electrode

$$Q = \frac{\tau_s}{r_2/D} \quad (7)$$

where τ_s is the stoichiometic discharge time, r the radius of the particle and D the chemical diffusion coefficient. Their analysis was developed for cathode materials, but we have adapted it here for Li^+-ion intercalation in graphite anodes. Substituting Eq. (6) in Eq. (7) yields

$$Q = \frac{1488D}{I_t B^2} \quad (8)$$

where τ_s is assumed to be equal to t_t, and the particle radius is taken to be equal to 1/2 the basal length of the flake-like natural graphite (i.e. B/2).

3.1. Experimental data

The intercalation of Li^+ ions, and the reversible capacity, was determined at different C-rates following the definition by the battery community, i.e. computed using Eq. (6). For instance, the C/24-rate corresponds to 15.5 mA/g, C/4-rate is equivalent to 93 mA/g and 2C rate corresponds to 744 mAh/g. The amount of Li^+ ions that intercalate (reversible capacity) at these rates is determined from measurement of the coulombic charge corresponding to de-intercalation of Li^+ ions.

The composition of intercalated graphite, x in Li_xC_6, that is obtained with natural graphite of different particle size is presented in Fig. 3 as a function of discharge rate. At low specific currents, the composition of lithiated graphite

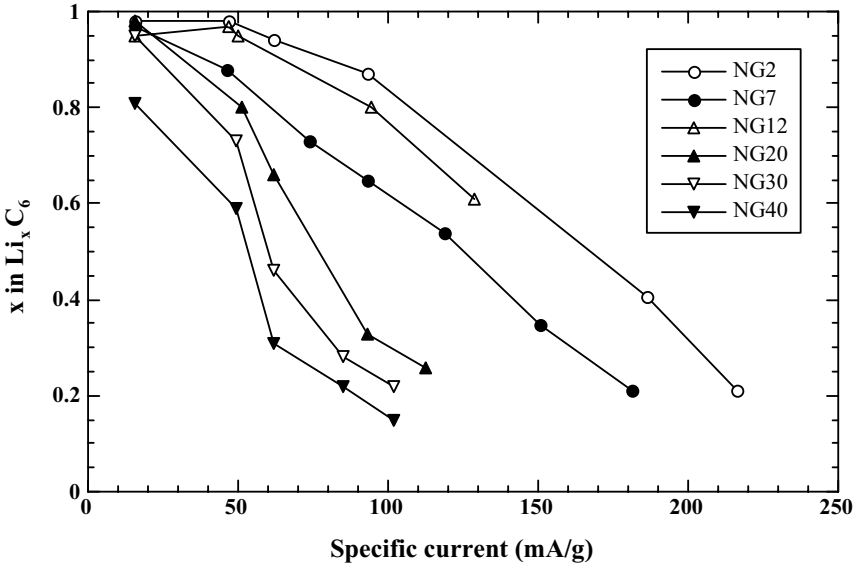

Fig. 3. Composition of intercalated graphites, x in Li_xC_6, vs. discharge rate of 2D natural graphite. Parameter is particle size.

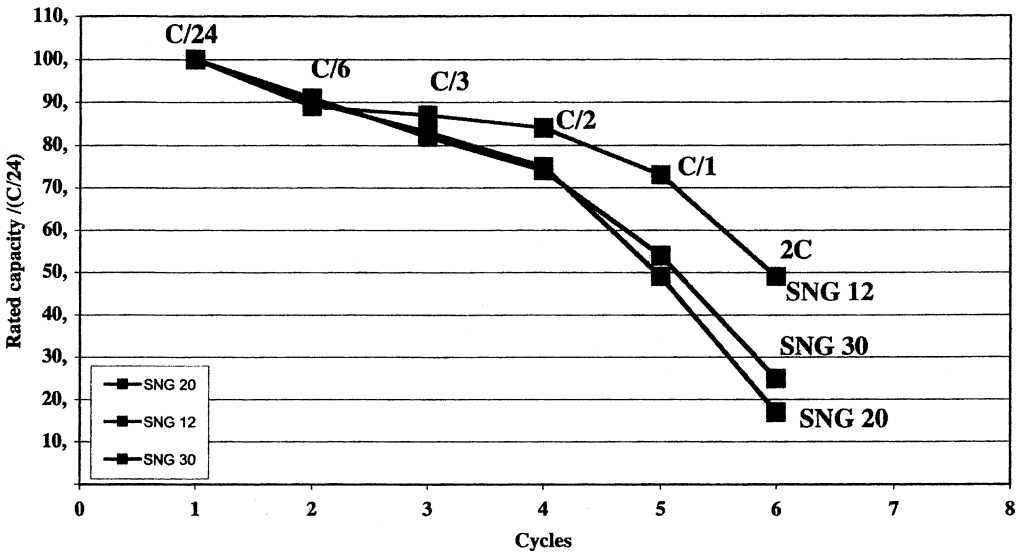

Fig. 4. Percent rated capacity $C/24$ (100% is equivalent to $x = 1$ in Li_xC_6) vs. discharge rate of 3D natural graphite. Parameter is particle size.

approaches the theoretical value, $x = 1$, except for natural graphite with the largest particle size. However, x decreases with an increase in specific current for all particle sizes. This trend suggests that solid-state diffusion of Li^+ ions is limiting the intercalation capacity in graphite. At this time, we have no good explanation for the higher reversible capacity of NG12 compared to NG7. The theoretical analysis by Dalard et al. [9] illustrated that the particle size distribution of the particles in an electrode has an influence on the electrode capacity at a given intercalation rate. The presence of a small fraction of large particles in a composite electrode with a majority of monodisperse small particles lowered the overall intercalation capacity. The particle size distribution of the natural graphite was not considered in the present study, but this factor could play a role in the scatter observed in the data.

The % rated capacity of 3D natural graphite of different particle size, which is normalized to the capacity at $C/24$ (372 mAh/g), is plotted in Fig. 4 as a function of discharge rate (specific current). At low specific currents, the composition of lithiated graphite is equal to $x = 1$, or 372 mAh/g. The % rated capacity decreases with an increase in specific current for all particle sizes. At specific current $> C/3$ SNG12 has the highest rate capability. At $C/3$, the capacity of SNG12 is 327 mAh/g while that of 2D graphite NG12 is 225 mAh/g. This trend suggests that solid-state diffusion of Li^+ ions is limiting the intercalation capacity in graphite. The higher reversible capacity of SNG12 compared to NG12

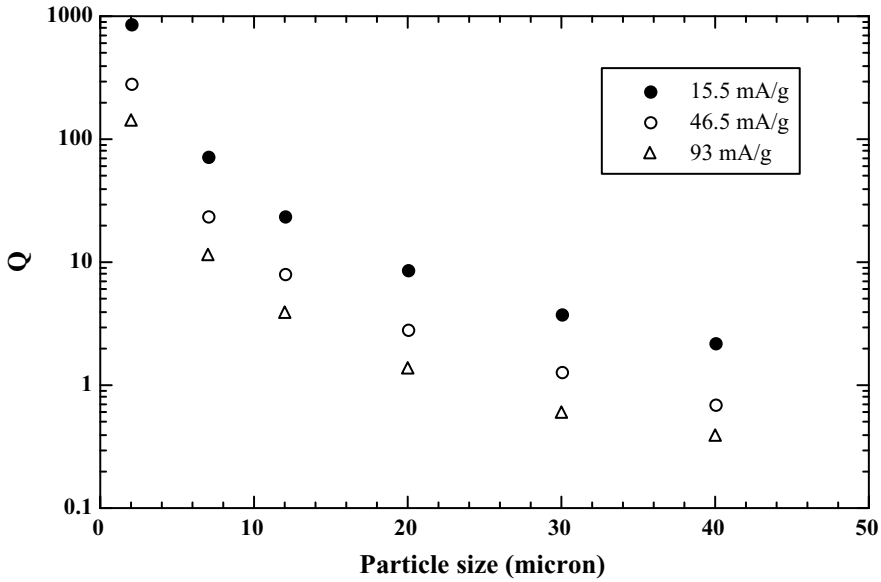

Fig. 5. Q as a function of particle size. Parameter is discharge rate.

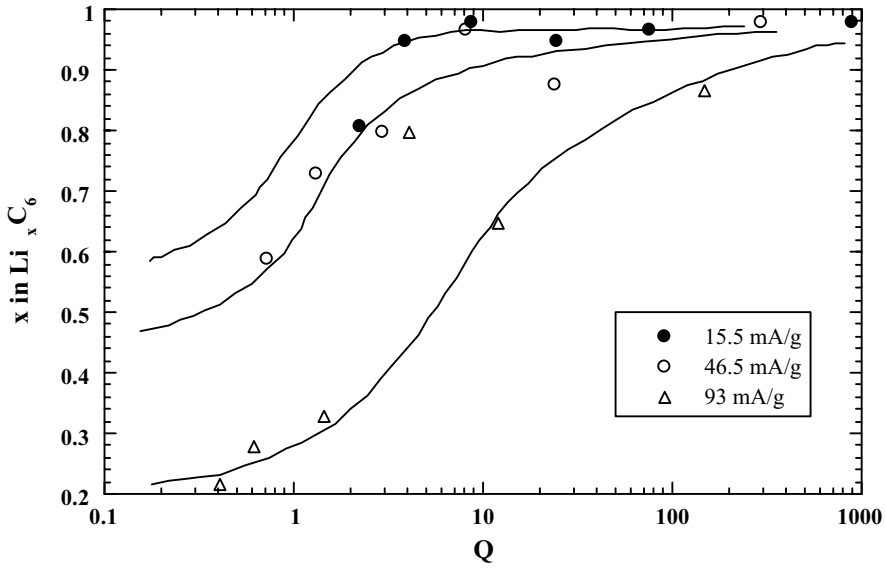

Fig. 6. Composition of intercalated graphites, x in Li_xC_6, vs. Q. Parameter is discharge rate. Lines indicate trend of the data following the analysis of Atlung et al. [8].

at high rates may indicate the important role of edge sites. For the particles with a three-dimensional morphology, the edge fraction f_e [3] is higher than f_e for the two-dimensional morphology, which facilitates rapid solid-state diffusion of Li^+ ions.

Atlung et al. [8] defined a parameter Q (see Eq. (8)), which was applied to analyze the rate dependence of Li^+-ion intercalation in flake natural graphite. A solid-state diffusion coefficient of 10^{-10} cm^2/s was used in Eq. (4), which is consistent with the values reported by Yu et al. [7] for Li^+-ion diffusion in graphite (i.e. 1.12×10^{-10} to 6.51×10^{-11} cm^2/s for 0 and 30% state of charge at 25 °C, respectively). These results are presented in Fig. 5 for Q as a function of particle size and at three discharge currents. The value of Q decreases with an increase in the particle size, and it is lower at higher discharge rate. The utilization and coulombic efficiency of the discharged electrode can be correlated to Q. As the particle size increases, Q decreases and the coulombic efficiency decreases. Thus, the coulombic efficiency for graphite of a given particle size is lower at higher discharge rates. If a diffusion coefficient of 10^{-8} cm^2/s is used in the analysis instead of 10^{-10} cm^2/s, the net effect would be to increase Q by a factor of 100.

Fig. 6 shows plots of x as a function of Q. Lines that illustrate s-shaped curves are drawn to follow the trend for coulombic efficiency versus $\log Q$ presented by Atlung et al. [8]. When $x = 1$, the maximum capacity for intercalation of Li^+ ions in graphite is obtained, and the coulombic efficiency is 100%. The intercalation capacity decreases with a decrease in Q and an increase in discharge rate. The low coulombic efficiency is most notable for $Q < 10$, particularly at a discharge rate of 93 μm. Referring to Fig. 5, it is evident that $Q < 10$ corresponds to particle sizes larger than 10 μm where limitations in solid-state diffusion have a strong influence on the intercalation capacity.

4. Concluding remarks

The intercalation of Li^+ ions in graphite electrodes in nonaqueous electrolyte involves transport of the ions in the liquid phase to the edge plane sites, followed by solid-state diffusion between the layer planes. Analysis of these processes indicates that solid-state diffusion limits the capacity of graphite to intercalate Li^+ ions at high intercalation rates. The particle size also plays a role in the reversible intercalation capacity of graphite. At low specific current (15.5 mA/g carbon), the composition of lithiated graphite approaches the theoretical value, $x = 1$ in Li_xC6, except for the natural graphite with the largest particle size. However, x decreases with an increase in specific current for all particle sizes for 2D and 3D graphite, suggesting that solid-state diffusion of Li^+ ions limits the intercalation capacity in graphite. Analysis of the area of edge sites and the intercalation current showed no dependence on particle size. This finding indicates that the transport of Li^+ ions in the electrolyte does not limit the intercalation capacity.

The highest reversible capacity of Li^+ ions is achieved with the smallest particles of flake natural graphite in our study. However, the irreversible capacity loss (ICL), which involves electrolyte decomposition and the formation of the so-called SEI layer, increases with a decrease in particle size (increase in surface area) of graphite [2,15–21]. Furthermore, the ICL is strongly affected by the relative amounts of basal plane and edge sites, with the edge sites being the more active (catalytic) sites for electrolyte decomposition [2]. Yazami [22] obtained a first-order approximation for

the relationship between the reversible capacity (372x, x in Li_xC_6) and ICL:

$$372x = 381 - 0.73\text{ICL} \quad (9)$$

From this relationship, the cycle efficiency (CE)

$$\text{CE} = \frac{372x}{372x + \text{ICL}} \quad (10)$$

after substitution of Eq. (9) is given by

$$\text{CE} = \frac{372x}{381 + 0.27\text{ICL}} \quad (11)$$

It is apparent from Eq. (11) that an increase in ICL has an adverse effect on the cycle efficiency of Li-ion cells during the early cycles. Furthermore, if x is reduced by high discharge rates, the net result is a lower specific energy. Mixtures of carbons with different average particle size were not considered in our study, but they could provide improved intercalation capacity in negative electrodes for Li-ion cells [23]. The recent study by Claye et al. [24] demonstrated that high reversible capacity (405 mAh/g) for Li intercalation is feasible at high rate (186 mA/g or C/2-rate) with single-wall carbon nanotubes (SWNT). Unfortunately, the SWNT has a high irreversible capacity loss (1200 mAh/g). The small particle size (10–50 nm diameter and several microns in length) of SWNT facilitates high Li^+-ion intercalation rates, but the corresponding high surface area (350 m^2/g) is not compatible with low ICL. Clearly, a compromise in the particle size and surface area, as well as particle morphology/structure (e.g. Huang et al. [25] demonstrated the difference in rates with graphite and coke at low temperature), is needed to obtain the optimum performance at high charge–discharge rates of graphite. However, for the particles with a three-dimensional morphology, the edge fraction f_e is higher than f_e for the two-dimensional morphology which gives a rapid solid-state diffusion of Li^+ ions. These results suggest that the three-dimensional graphite morphology is more suitable for Li-ion batteries requiring high-rate charge–discharge such as in HEV. The 3D natural graphite with a particle size of 12 μm may provide the optimum combination of reversible capacity (327 mAh/g at 124 mA/g) and irreversible capacity loss (40 mAh/g) in the electrolyte and discharge rates used in this study.

Acknowledgements

The authors would like to acknowledge the support of HydroQuébec and the Assistant Secretary for Energy Efficiency and Renewable Energy, Office of Advanced Automotive Technologies of the US Department of Energy under Contract no. DE-AC03-76SF00098 at Lawrence Berkeley National Laboratory.

References

[1] K. Amine, J. Liu, A. Jansen, A. Newman, D. Simon, G. Henriksen, in: G. Nazri, M. Thackeray, T. Ohzuku (Eds.), Proceedings of the Symposium on Intercalation Compounds for Battery Materials, The Electrochemical Society, Inc., Pennington, NJ, vol. 99-24, 2000, p. 389.
[2] K. Zaghib, G. Nadeau, K. Kinoshita, J. Electrochem. Soc. 147 (2000) 2110.
[3] W. Jiang, G. Nadeau, K. Zaghib, K. Kinoshita, Thermochim. Acta 351 (2000) 85.
[4] M. Verbrugge, B. Koch, J. Electrochem. Soc. 146 (1999) 833.
[5] M. Verbrugge, B. Koch, J. Electrochem. Soc. 143 (1996) 600.
[6] T. Fuller, M. Doyle, J. Newman, J. Electrochem. Soc. 141 (1994) 1.
[7] P. Yu, B. Popov, J. Ritter, R. White, J. Electrochem. Soc. 146 (1999) 8.
[8] S. Atlung, K. West, T. Jacobsen, J. Electrochem. Soc. 126 (1979) 1311.
[9] F. Dalard, D. Deroo, D. Foscallo, J. Merienne, J. Power Sources 14 (1985) 209.
[10] T.D. Tran, J.H. Feikert, R.W. Pekala, K. Kinoshita, J. Appl. Electrochem. 26 (1996) 1161.
[11] M. Fujimoto, Y. Shouji, T. Nohma, K. Nishio, Denki Kagaku 65 (1997) 949.
[12] A. Funabiki, M. Inaba, Z. Ogumi, S. Yuasa, J. Otsuji, A. Tasaka, J. Electrochem. Soc. 145 (1998) 172.
[13] Z. Zhang, in: S. Megahed, B. Barnett, L. Xie, (Eds.), Proceedings of the Symposium on Rechargeable Lithium and Lithium-Ion Batteries, The Electrochemical Society, Inc., Pennington, NJ, vol. 94-28, 1994, p. 165.
[14] Q. Liu, T. Zhang, C. Bindra, J. Fischer, J. Josefowicz, J. Power Sources 68 (1997) 287.
[15] G.-C. Chung, S.-H. Jun, K.-Y. Lee, M.-H. Kim, J. Electrochem. Soc. 146 (1999) 1664.
[16] M. Winter, P. Novak, A. Monnier, J. Electrochem. Soc. 145 (1998) 428.
[17] E. Buiel, A. George, J. Dahn, J. Electrochem. Soc. 145 (1998) 2252.
[18] E. Buiel, J. Dahn, J. Electrochem. Soc. 145 (1998) 1977.
[19] M. Fujimoto, K. Ueno, T. Nohma, M. Takahashi, K. Nishio, T. Saito, in: B. Barnett, E. Dowgiallo, G. Halpert, Y. Matsuda, Z. Takehara (Eds.), Proceedings of the Symposium on New Sealed Rechargeable Batteries and Supercapacitors, The Electrochemical Society, Inc., Pennington, NJ, vol. 93-23, 1993, p. 281.
[20] T. Iijima, K. Suzuki, Y. Matsuda, Synth. Met. 73 (1995) 9.
[21] K. Tatsumi, K. Zaghib, Y. Sawada, H. Abe, T. Ohsaki, J. Electrochem. Soc. 142 (1995) 1090.
[22] R. Yazami, Electrochem. Acta 45 (1999) 87.
[23] Y. Sato, T. Nakano, K. Kobayakawa, T. Kawai, A. Yokoyama, J. Power Sources 75 (1998) 271.
[24] A. Claye, J. Fischer, C. Huffman, A. Rinzler, R. Smalley, J. Electrochem. Soc. 147 (2000) 2845.
[25] C.K. Huang, J. Sakamoto, J. Wolfenstine, S. Surampudi, J. Electrochem. Soc. 147 (2000) 2893.